New limits of sensitivity of site-directed spin labeling electron paramagnetic resonance for membrane proteins

Bordignon, Enrica; Bleicken, Stephanie

How to cite

BORDIGNON, Enrica, BLEICKEN, Stephanie. New limits of sensitivity of site-directed spin labeling electron paramagnetic resonance for membrane proteins. In: Biochimica et biophysica acta. Biomembranes, 2018, vol. 1860, n° 4, p. 841–853. doi: 10.1016/j.bbamem.2017.12.009

This publication URL: https://archive-ouverte.unige.ch/unige:173913
Publication DOI: 10.1016/j.bbamem.2017.12.009

BBA - Biomembranes 1860 (2018) 841–853

Contents lists available at ScienceDirect

BBA - Biomembranes

journal homepage: www.elsevier.com/locate/bbamem

Review

New limits of sensitivity of site-directed spin labeling electron paramagnetic resonance for membrane proteins☆

Enrica Bordignon*, Stephanie Bleicken

Faculty of Chemistry and Biochemistry, Ruhr University Bochum, Universitaetsstrasse 150, 44801 Bochum, Germany

ARTICLE INFO

Keywords:
EPR
Nitroxide
Spectroscopy
Dynamics
Water accessibility
Distances

ABSTRACT

Site-directed spin labeling electron paramagnetic resonance is a biophysical technique based on the specific introduction of spin labels to one or more sites in diamagnetic proteins, which allows monitoring dynamics and water accessibility of the spin-labeled side chains, as well as nanometer distances between two (or more) labels. Key advantages of this technique to study membrane proteins are addressed, with focus on the recent developments which will expand the range of applicability. Comparison with other biophysical methods is provided to highlight the strength of EPR as complementary tool for structural biology. This article is part of a Special Issue entitled: Beyond the Structure-Function Horizon of Membrane Proteins edited by Ute Hellmich, Rupak Doshi and Benjamin McIlwain.

1. Introduction

All living organisms depend on membranes confining individual cells and the compartments/organelles within [1,2]. Thereby, approximately 30% of the human proteins are membrane-embedded or membrane-attached. Membrane proteins receive signals from outside the cell and translate them into intracellular action, enable a controlled exchange of material, information and energy across the membranes, as well as shape, stabilize, fuse or divide membranes, organelles and cells. However, compared to soluble proteins, our knowledge on the structure, function and interactions of membrane proteins in their native environment is still limited, as many experiments face technical limitations.

This review describes the defining aspects of site-directed spin labeling (SDSL) electron paramagnetic resonance (EPR) spectroscopy, a technique which can be applied without size or environment limitations to membrane proteins, providing with a high level of fidelity and sensitivity site-specific information about dynamics, water accessibility and relative location of spin-labeled probes covalently attached to proteins. In contrast to NMR, which shares with EPR the basic quantum mechanical description but relies on the detection of the complex interaction network of a variety of intrinsic nuclear spins isotopes (^{1}H, ^{2}H, ^{13}C, ^{14}N, ^{15}N, ^{31}P…), SDSL EPR requires in most cases the introduction of ad hoc spin labels carrying unpaired electrons. Naturally occurring electron spin centers also exist in proteins carrying metal cofactors, or if short-living radical species are created during a reaction, but these cases are not covered in this review. Site-specificity implies that one (or few) sites can be labeled and analyzed for each protein. This conveys both the major advantage of the technique in terms of specificity, sensitivity and negligible size/environment limitations, as well as its major disadvantage, i.e. it cannot provide protein structures at atomic resolution, but rather coarse-grained structural models.

SDSL EPR was introduced by the pioneering work of Hubbell in the 1990's (notably, one the first studied proteins was a membrane protein [3]) and it has now become a wide spread complementary tool in structural biology.

In the following, we describe the main information that can be obtained by SDSL EPR on membrane proteins, namely dynamics of the spin-labeled side chain, water/membrane accessibility and interspin distances. Breakthrough technical innovations will be highlighted in each paragraph, to provide a state-of-the-art answer to the question: “Can I use SDSL EPR to gain structural insights on my favorite membrane protein, and which information can I obtain?”. At the end, we will provide two examples of EPR studies from our lab performed on Bax, a propapoptotic human protein and on TM287/288, a bacterial ABC exporter.

2. The starting point: mutagenesis and labeling

First, we need to attach one (or few) spin label(s) to specific sites in a protein. The most common strategy is to utilize cysteines engineered at defined positions, and covalently attach a nitroxide label via different

☆ This article is part of a Special Issue entitled: Beyond the Structure-Function Horizon of Membrane Proteins edited by Ute Hellmich, Rupak Doshi and Benjamin McIlwain.

* Corresponding author.
E-mail address: enrica.bordignon@rub.de (E. Bordignon).

https://doi.org/10.1016/j.bbamem.2017.12.009
Received 12 July 2017; Received in revised form 27 November 2017; Accepted 9 December 2017
Available online 14 December 2017
0005-2736/

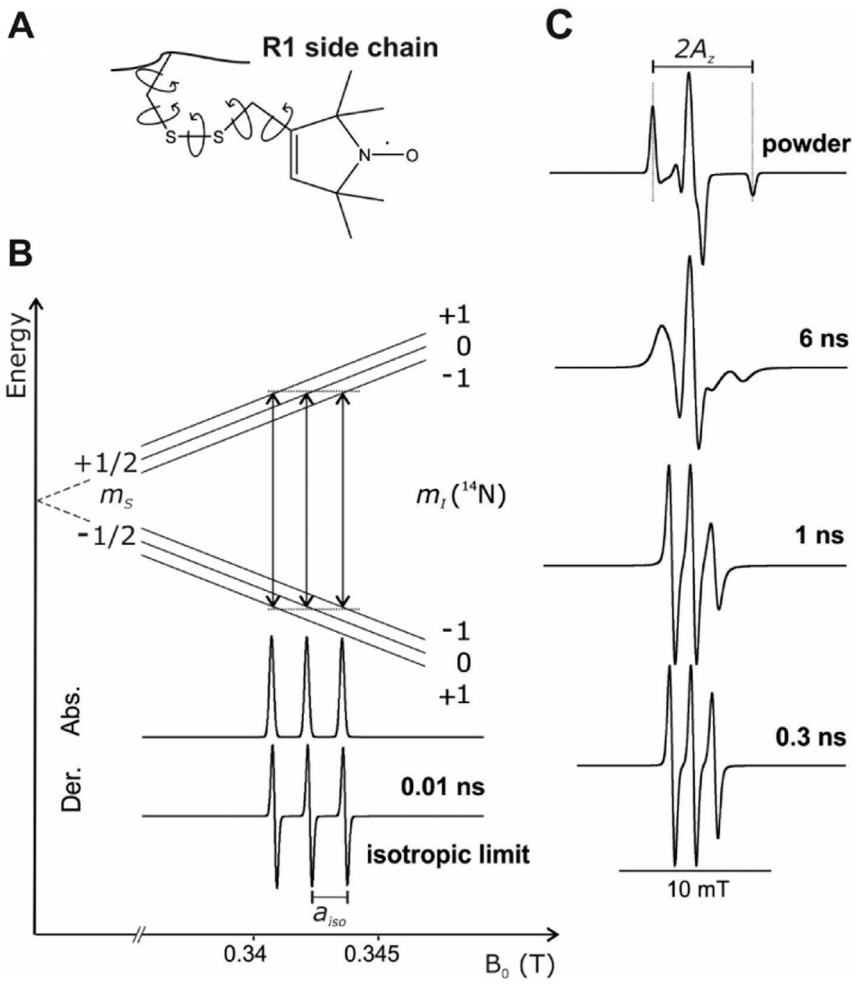

Fig. 1. Nitroxide probes and dynamics encoded in the spectral lineshape. **A**) Scheme of an MTSL probe bound to a cysteine residue. The five rotatable bonds are highlighted. B) Energy scheme showing the origin of the three-line spectrum for a nitroxide in the isotropic fast motion limit. The rotational correlation time used for the spectral simulation is 10 ps (simulation done with Easyspin [16]). The upper spectrum is the X-band absorption, the bottom one is the derivative. CW EPR spectra are usually detected via lock-in detection, therefore they are presented as derivative spectra. C) Example of X-band spectra with different rotational correlation times (written in the figure legend). The first is the 'powder' spectrum in the absence of molecular motion (powder or frozen samples); the distance between the low and high field peak is the $2A_z$ hyperfine component. The other spectra show the effects of rotational motion on the spectral features. Faster motions are characterized by narrower lines and higher intensity of the third line with respect to the central one.

functional groups [4]. Therefore, it follows that the membrane protein of interest should ideally contain no natural cysteines, or eventually only few which are not accessible to the label. In general, natural cysteines are removed and, if this is not impairing protein function and structure, one can start to introduce one cysteine at a time. If functionally relevant cysteines are present, one can try to circumvent the problem by producing a protein incorporating unnatural amino acids which can either react specifically with a functionalized nitroxide probe or directly carry a nitroxide label (see for example [5,6]), which for membrane proteins remains a challenging task, because it requires much more effort than conventional recombinant protein purification methods. Otherwise, an alternative possibility is to attach a nitroxide spin probe to a tyrosine residue, which was shown to be effective and specific [7].

The most common spin label for cysteines is a methanethiosulfonate functionalized nitroxide radical (MTSL, (1-Oxyl-2,2,5,5-tetramethyl-Δ3-pyrroline-3-methyl) methanethiosulfonate), which carries a stable spin ½ delocalized in the N-O bond (Fig. 1A) and targets engineered cysteine residues in proteins with high specificity. However, the labeling efficiency (how many cysteines carry the nitroxide label) is site-specific, and it can reach 100% for exposed sites, but can also be close to 0% for sites buried in the protein interior. Thus, pre-knowledge of the possible water exposure of the engineered site favours the success of the SDSL EPR study. Due to its high specificity for cysteines and good degree of labeling, MTSL is the right choice if one wants to extract information on the dynamics of a protein site at physiological temperature. This spin label is inert at most positions and a large amount of data exist in literature, which facilitates data analysis and comparison. Due to the diamagnetic nature of the non-labeled proteins, the EPR signal arises only from the fraction of labeled variants in the ensemble. Therefore, for mobility and water accessibility studies, low labeling efficiencies are not detrimental for data analysis, but only if it is possible to ascertain the correct fold and functionality of the spin-labeled fraction in the ensemble. In case the labile nature of the S-S bond between the cysteine and the label causes problems, other types of labels functionalized with maleimido or iodacetamido groups are commercially available, which are linked to the protein via a more stable S-C bond. If reducing environments cannot be avoided, a series of sterically protected nitroxide labels are also available (for a recent review on nitroxide labels see [8]).

Besides nitroxide probes, many other spin labels were recently introduced, especially for interspin distance measurements. Examples are: functionalized chelators of paramagnetic lanthanides (Gd^{III}, spin 7/2) reacting with cysteines (for a review see [9]); carbon-based radicals (trityl, spin ½) [10] targeting cysteines; metals such as copper (Cu^{II}, spin ½) which specifically bind to engineered high-affinity histidine binding sites in proteins [11]. Despite specific advantages, which will be introduced later, the latter probes are spectroscopically orthogonal to nitroxides, meaning that they can be distinguished by spectral absorption, relaxation times, detection schemes, etc. Therefore, if protein oligomers or multiprotein complexes are labeled with distinct probes, simultaneous extraction of interspin distances between different pairs in the same sample is possible (e.g. Gd-Gd, Gd-nitroxide, Cu-nitroxide, etc.). In the last few years, several new spectroscopically orthogonal spin label pairs and distance measurements were reported (see paragraph "Interspin distances" below). The biggest disadvantage of the Gd-based and trityl labels is that they are bulkier than nitroxide probes and labeling site must be chosen with care to avoid interference in protein

structure and function. Their introduction into membrane proteins has not yet become a routine, however interesting examples of successful applications can already be found in literature (see for example [12–15]).

3. Dynamics and water/membrane accessibility

Information about the dynamics of the spin-labeled side chain at physiological temperature can be extracted when nitroxide probes are used, because the spectral shape encodes the speed and amplitude of its characteristic reorientational motion (Fig. 1). The three-line continuous wave (CW) EPR spectrum of a freely tumbling nitroxide in water (Fig. 1B) arises from the hyperfine coupling between the electron spin ½ and the ^{14}N (nuclear spin 1).

Due to the anisotropic nature of the hyperfine interaction, the strength of the coupling (splitting between the three spectral lines) depends on the orientation of the nitroxide molecule with respect to the external magnetic field. Due to the small g anisotropy, the hyperfine anisotropy dominates the spectra at low fields. The rotation correlation time of the molecular motion will modulate the appearance of the nitroxide spectrum. In conventional X-band CW EPR (0.34 T magnetic field, 9.5 GHz microwave excitation), the narrower the central line of the derivative spectrum, the faster the motion (Fig. 1B,C). Line broadening and appearance of the positive and negative peaks respectively in the low and high field region of the CW spectrum indicate lower mobility of the nitroxide molecule (Fig. 1C). When molecular motions are blocked, e.g. by freezing the sample, the 'powder' spectrum is detected, which contains the sum of the spectra over all possible molecular orientations and has a recognizable lineshape, shown in Fig. 1C. When MTSL is attached to a protein site (Fig. 1A) via its linker containing five rotatable bonds, it will have a specific spectral shape, which is determined by the reorientational freedom of the linker, modulated by the protein secondary, tertiary and quaternary interactions and by the intrinsic dynamics of the backbone. Lineshape analysis provides information on the distinct dynamics of each labeled site in a protein.

Conventional X-band spectra (Fig. 1) are still the most useful qualitative indicators of mobility (the EPR mobility parameter is just the inverse of the central linewidth of the spectrum [4]), especially for membrane proteins. However, a quantitative description of the complex molecular motion encoded in the EPR lineshape requires a multifrequency approach, as pioneered by Freed (see for example [17]). In fact, going to higher fields/frequencies (for example Q band, 1.2 T, 35 GHz or W band, 3.4 T, 95 GHz) allows to disentangle the anisotropies of the rhombic g tensor of nitroxides, due to higher Zeeman resolution. Additionally, faster motions (< 0.5 ns) are better resolved at high fields due to an increased spectral width.

CW EPR is a rather sensitive and fast technique, and it requires about 20 µl of a minimum of 5–10 µM spin concentration for membrane proteins spin-labeled with nitroxide probes (Fig. 1A). In general, a CW spectrum can be detected in a few minutes and signal averaging can take up to 1 h, depending on the spin concentration. The sample can be completely recovered after the EPR scan.

A site scan, namely the addition of one nitroxide per amino acid in a protein region, enables monitoring the dynamics of neighboring side chains thereby highlighting a possible periodical pattern. The latter is a useful indicator for helicity (3.6 periodicity) or beta sheet (2 periodicity) and, together with water accessibility data (see below), can be an effective secondary structure validation tool providing, for example, insights into the topology of an amphipathic helix with respect to the membrane-water boundaries (one example can be found here [18]). A more straightforward application is the analysis of the changes in mobility of one spin-labeled site in different conformations of the protein, upon translocation of a protein from the water to the membrane (Fig. 2A), upon ligand binding or interaction with a protein partner. In this case, the mobility of each site reports on the local rearrangements around the spin probe.

A technical development which we want to highlight and that will impact the studies of membrane proteins is rapid scan acquisition, pioneered by the Eatons' lab [19–21]. In general, the low yield of membrane proteins poses limits in the maximum concentration achievable and, most importantly, many protein-protein interactions happen physiologically at concentrations well below micromolar. Although conventional CW EPR phase sensitive detection allows to measure few micromolar spin concentrations (Fig. 2A), a gain of a factor 10 could push the field towards measuring protein dynamics and interactions in the high nanomolar range. Rapid scan EPR has proven to provide such an increase in signal to noise. The setup requires additional components with respect to a CW EPR spectrometer, but its implementation will certainly enable new *in vitro* and *in vivo* applications on membrane proteins.

For these systems, the water-membrane boundaries are important descriptors of their topology. For standard transmembrane proteins, it is relatively easy to define the structural regions in contact with the lipids. In contrast, for peripheral proteins or proteins shuttling from the cytosol to the membranes, prediction of the membrane boundaries is difficult. EPR offers the possibility to monitor the water accessibility of each spin-labeled site in a protein. One available conventional technique is based on the analysis of CW power saturation curves in the presence of paramagnetic relaxing agents soluble in water (NiEDDA) or in lipids (O_2). This technique enables disentangling water-exposed from lipid-exposed or protein buried sites, based on the differential change in the relaxation of the nitroxide labels (reviewed in [22]). The technique has high sensitivity and low sample volumes are required (< 10 µl), however, the sample is modified by the treatment (e.g. by addition of NiEDDA), the accessibility towards water is only indirectly measured through relaxation agents and the reproducibility level is medium.

Another common approach is to perform ESEEM (Electron Spin Echo Envelope Modulation) at cryogenic temperature. Here, deuterated glycerol or water is added to the sample, and the amount of deuterons close to the spin label is determined, which refers to how well the attached spin label is accessible to the bulk water and thus gives information on the topology with respect to the water-membrane boundaries (see for example [26–28]). Disadvantages are that this technique requires freezing of the sample, and it indirectly measures the water molecules, offset by the unknown number of exchangeable protons in the proteins.

With a frozen protein sample, it is also possible to obtain the *z* component of the hyperfine tensor *A* from X-band CW EPR (see for example Fig. 1C and 2B) or additionally extract the *x* component of the *g* tensor from high field CW EPR (95 GHz). Both values are sensitive to the polarity of the microenvironment of the nitroxide and g_x reports also the number of possible H-bonds towards the NO group (reviewed in [8]). At least 50 µM protein concentrations are required, and the thermal history of the sample needs to be controlled for reproducibility issues [29].

The limits of the previously mentioned approaches (frozen solutions and/or indirect detection of water molecules) can be overcome by X-band ODNP (Overhauser Dynamic Nuclear Polarization), an emerging technique to extract water accessibility data for membrane proteins. Briefly, in this experiment we monitor directly the change in the intensity of the FID (free induction decay) signal of the protons in the water molecules upon irradiating the coupled electron spins (e.g. nitroxide spin labels attached to the protein) with increasing microwave power [30]. The motion of the water molecules coupled via hyperfine interactions to the electron spins is responsible for the modulation of the relaxation properties at the basis of the Overhauser effect. The higher the ODNP enhancement (normalized to the electron spin concentration), the higher is the number of water molecules diffusing around the spin labels. The local diffusion of the water molecules can be extracted via model-based approaches from ODNP data [31], otherwise a more qualitative accessibility parameter can be extracted by comparing the enhancement at microwave powers up to 100 mW [25].

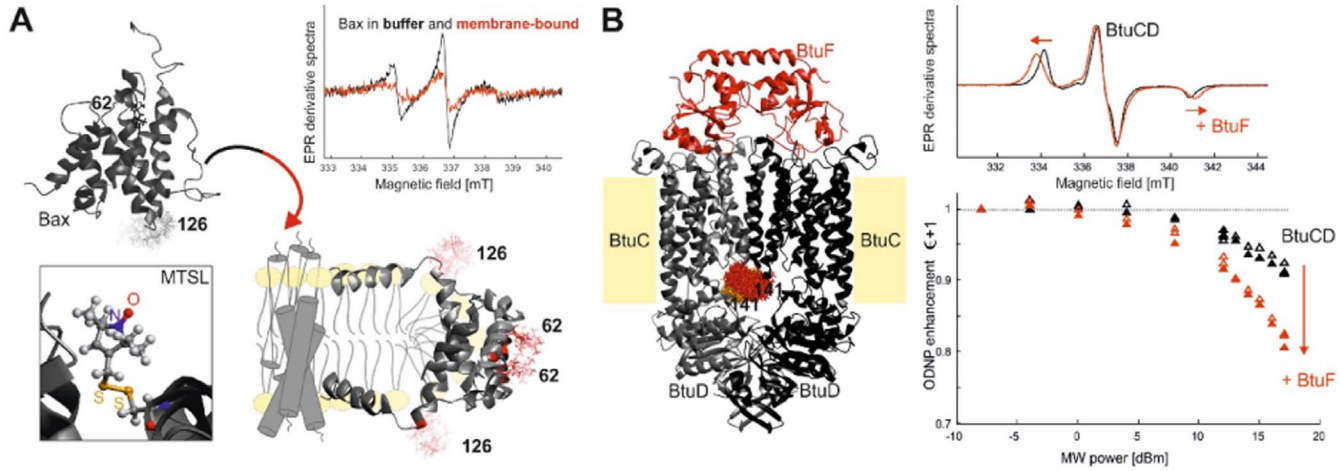

Fig. 2. Continuous wave EPR and ODNP on membrane proteins. **A**) The apoptotic protein Bax is spin labeled at the two natural cysteines (C62 and C126). The X-band EPR spectrum is recorded when the protein is an inactive monomer in water buffer (black spectrum in the upper inset) and after oligomerization and membrane insertion (red spectrum). The spectra are detected at 37 °C on the same sample at the beginning and at the end of a 4-hour incubation period within the resonator. Setup used: Bruker E580 spectrometer equipped with a SHQ cavity, modulation amplitude 0.15 mT, microwave power 9.5 mW, 4 scans, acquisition time 82 s, protein concentration 8 μM, spin concentration 15 μM. The conformational change of Bax is schematically shown in the panel. The water soluble Bax is the NMR structure (PDB ID: 1F16), the dimeric model is an EPR-derived structure taken from [23]. Both structures are spin labeled with MTSL using the room temperature rotamer library of the software MMM [24]. The structure of the MTSL bound to position 62 is highlighted in the box at the bottom left. **B**) The apo structure of the ABC importer BtuCD-F in its apo form is shown with the spin-labeled rotamers attached to sites 141 (cytoplasmic gate) in each unit (red and orange rotamers). Upon binding of BtuF (substrate binding protein) to the periplasmic side of the transporter, there is an evident change in polarity around the spin labels, seen as increase of the A_z component of the hyperfine tensor in the CW EPR spectra detected at 160 K (increased distance between the low and high field peaks going from the black to the red spectrum in the upper inset). The increased polarity correlates with an increased water accessibility, as judged from the increased effect on the intensity of the FID of the proton NMR signal at high microwave (MW) power (bottom inset, adapted from [25]). The ODNP sample contained 10 μM protein reconstituted in liposomes, extruded through 400 nm pores.

ODNP experiments have the advantages that it is possible to work with low volumes (few microliters) and low spin concentrations (down to 10 μM) at physiological temperature, and to directly quantify the amount of water molecules surrounding the labeled site. Monitoring changes in conformation of membrane proteins becomes feasible in a relative short amount of time (an ODNP experiment can take < 20 min [32]), therefore it is possible to monitor the kinetics of slow conformational changes. An example of ODNP application to an ABC transporter is shown in Fig. 2B.

4. Interspin distances

Determining interspin distances in proteins and protein complexes is the most appealing SDSL EPR tool for protein studies. It attracts the interest of the structural biology community because it allows mapping a network of distances between engineered sites in a protein, and monitoring their changes during proteins' function. In the last few years, thanks to advances in microwave technology, pulse manipulation techniques, new pulse schemes and novel spin labels, this field has seen an exponential growth, which led to a dramatic increase in sensitivity and reliability of the extracted distances for a large range of applications (especially for membrane proteins). Until 17 years ago, the mean distance between two nitroxide spin labels attached to a protein was solely detectable via convolution of low temperature continuous wave EPR spectra. In fact, dipolar broadening becomes visible if two probes are in close contact (< 2 nm). This limited the application of such technique to closely interacting spin pairs (for a comprehensive review of available methods and limitations see [33]). The introduction of a dead-time free 4-pulse Double Electron Electron Resonance (DEER) method in 2000 [34] and few years later of dedicated software for data analysis [35] opened the possibility to detect with high precision distance distributions longer than 1.5 nm. Therefore, distance constraints necessary to describe transmembrane regions of proteins (3–4 nm), o large protein complexes (5–10 nm) became experimentally available. Notably, the upper distance limit is defined by the relaxation properties of the probes, and by spin concentration sensitivity (16 nm is the longest detected distance so far measured with an 80 μs DEER trace [36]). The 4-pulse DEER experiment (also known as PELDOR, Pulse Electron Electron Double Resonance, Fig. 3A) is still the most widely used experiment to extract interspin distances on membrane proteins.

Here we will describe how the application of DEER to membrane proteins has become effective down to few tens of micromolar spins concentrations (in 40 μl of sample volume for Q-band resonators accepting 3 mm tubes). Until few years ago, X-band DEER was the prevalent technique used for protein studies and it required at least 100–200 μM concentrations for reliable distance extraction. Great advantages in terms of sensitivity were shown in 2012 by the use of Q-band spectrometers (34 GHz, 1.2 T magnetic fields) in combination with high power amplifiers (150 W). The amplifier allows the use of non-selective pulses (with about 100 MHz bandwidth), which minimize orientation section artefacts in the DEER traces [37]. This approach is still mostly used nowadays for nitroxide-labeled membrane proteins. Despite the increased sensitivity with respect to X band (20 fold in signal-to-noise, 400 fold in detection time), the reliability of the mean distance and the width of the distributions for membrane proteins is in general still limited by the fast transverse relaxation times of the spin labels due to proton spin diffusion (Fig. 3C). This is caused by the presence of hydrogens in the lipid chains in addition to those in the solvent and in the protein. Deuteration of solvents and proteins prolongs the relaxation times, and increases the quality of the data. However, replacing with deuterons the hydrogens in the lipid chains is not a trivial task (price and/or availability of the lipids are limiting factors). An additional drawback of membrane proteins in lipid bilayers is that there is a less homogeneous dispersion of proteins than in solution, which makes the decay of the DEER trace, which is related to intermolecular spin-spin contributions, more difficult to correct (Fig. 3C). The use of detergents or nanodiscs instead of liposomes alleviates the latter problem, but decreases the physiological relevance of the milieu. Despite the limitations described for membrane proteins, the increased sensitivity allows reliable distance determination with low protein concentrations (about 20–30 μM). Notably, the background decay of the DEER traces is less pronounced at low concentrations, therefore easier to correct, increasing the reliability of the distance information (Fig. 3C).

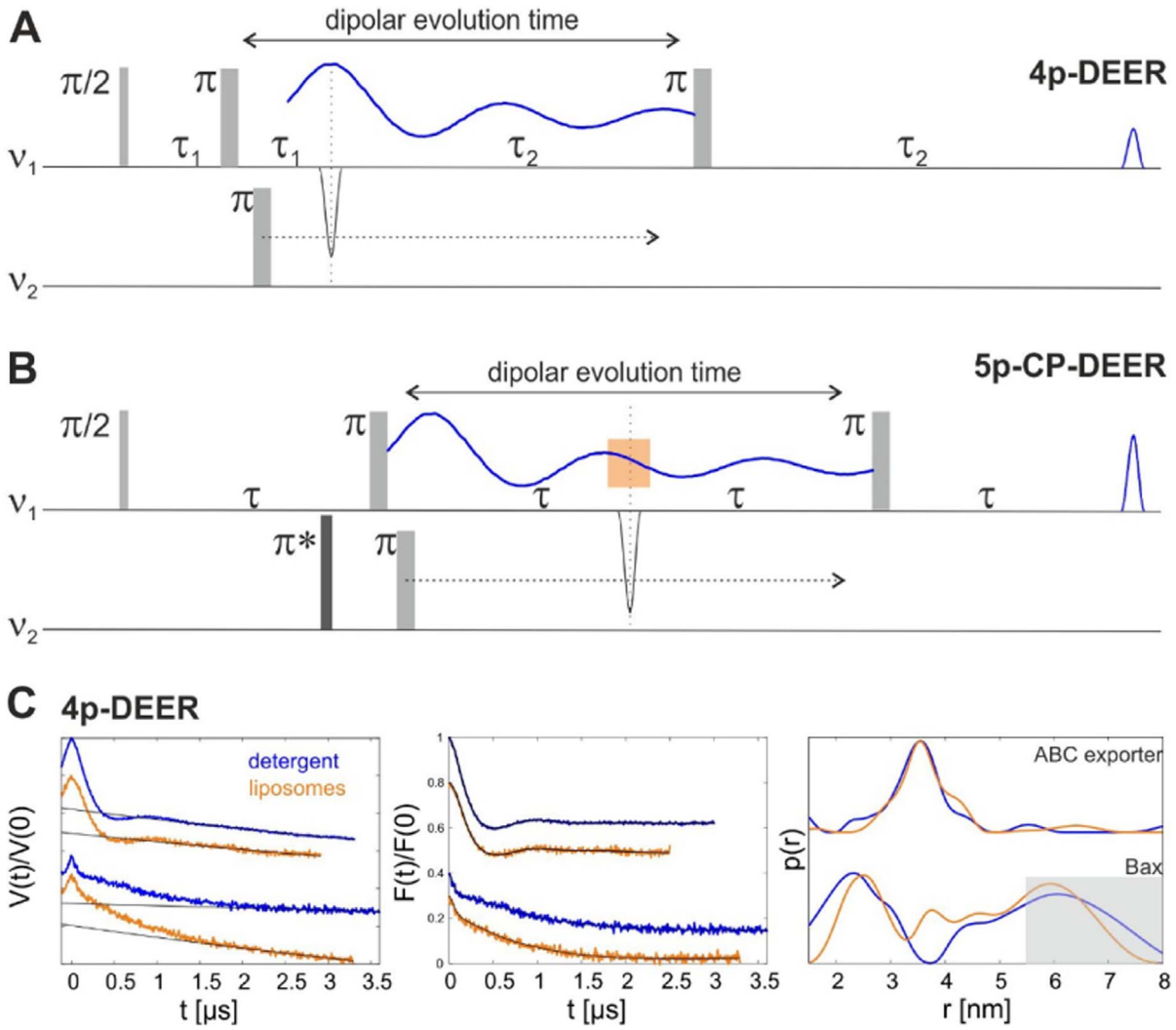

Fig. 3. Dipolar spectroscopy on membrane proteins. **A**) 4-pulse DEER pulse scheme. The first frequency (ν_1) excites a subpopulation of the spins in the sample (A spins); the second frequency (ν_2) excites another subpopulation (B spins). The π pulse at ν_2 moves within the dipolar evolution time window, and, as a result, the intensity of the refocused echo (highlighted in blue) is modulated with the dipolar interaction frequency (proportional to the inverse cubic power of the distance). Superimposed to the dipolar evolution time window, the expected modulation of the echo intensity (blue trace). **B**) 5-pulse Carr-Purcell (CP) DEER pulse scheme. The pulses at ν_1 are equally spaced (Carr Purcell scheme), therefore the loss of transverse magnetization is minimized, and the intensity of the refocused echo (cyan) is bigger than in the 4p-DEER at a given time after the first π/2 pulse of the sequence. This is the main advantage of this pulse scheme. To shift the phase of the sampled dipolar interaction, the additional, stationary pump pulse in the 5-pulse DEER setup (black pulse denoted with an asterisk) must invert the same spins as the time-variable pump pulse. This can be achieved with hard monochromatic rectangular pulses or with AWG-generated shaped pulses. The region on the time domain trace affected by partial excitation artefacts is highlighted in red. **C**) Examples of 4p-DEER traces detected for membrane proteins in detergent micelles (blue) or proteoliposomes (orange). The primary DEER traces are shown on the left, with the background fit. In membrane, the background usually deviates from a pure exponential and is decays faster than in detergents, therefore it is more difficult to correct it. To obtain similar signal-to-noise ratios as in detergent, shorter traces are recorded and averaged for a longer time (for example, the detergent traces can be acquired in 4–6 h, those in liposomes needs at least 12 h accumulation). In the middle panel the background corrected data are shown, with the fit (black) done with DeerAnalysis [35]. On the left the extracted distance distributions. For the ABC transporter TM287/288, a peak at 3.5 nm is detected with both preparations (spin labels located in TM288 at positions 131 and 248), with the same level of accuracy [38]. For the Bax sample embedded in membranes (labeled at position 62 and 186; spin diluted 1:3 with unlabeled Bax) [23], the shorter DEER trace and the steep background decay does not allow a reliable extraction of the mean distance and the width of the long component. The grey square denotes the region of decreased reliability of the data (based on distance validation using tools in DeerAnalysis). Prolonging the dipolar evolution time with CD-5p-DEER will help increasing the detection sensitivity in this sample.

So far, we have described only the detection of one interspin distance between two spin labels engineered in a macromolecule. For membrane proteins, this situation is encountered if the doubly-labeled protein under investigation is monomeric, or if we detect the interaction between two singly-labeled proteins in a dimeric complex. However, homo- and hetero- complexes are physiologically relevant. When such complexes are studied by EPR, more than two spins interact, and the true distance distributions contains all pairwise contributions, as well as “ghost peaks” due to combination of dipolar frequencies in DEER experiments [39]. Extracting each true distance reliably by DEER is possible if the flipping angle of the pump pulse is decreased and if unlabeled proteins are introduced in the sample (spin dilution methods) (see for example [23,40–42]). To reduce the complexity of the spin system and of data analysis, orthogonal labeling can also be used, as described in the following.

One recent advance in the field of EPR spectroscopy is the use of arbitrary waveform generators (AWG), which allows to manipulate amplitude, phase and frequency of the irradiating microwave fields, therefore enabling to tailor the excitation bandwidth of the microwave pulses to the available spin systems. New AWG-based sequences are being developed (for recent reviews see [43–45]) and will reshape the state-of-the-art techniques for SDSL EPR in the following years, especially when metal-based labels are employed.

Among the various AWG-based methods which are being developed,

we choose to focus on the 5-pulse DEER experiment as example of technical innovation in the field of dipolar spectroscopy for membrane proteins. In fact 5-pulse DEER can improve the detection reliability of long interspin distances at low protein concentration, which are the two main challenging issues when membrane proteins are studied in native environments. The first 5-pulse version of DEER was introduced by Borbat et al. [46]. It explores the use of a Carr Purcell train pulse scheme to decrease the effects of spin diffusion on the transverse relaxation (T_2*) of the electron spins (Fig. 3B), thereby prolonging their transverse relaxation time. As a consequence, longer dipolar evolution times become accessible, which has a profound impact in the upper limit of distances which can be reliably detected with DEER, and in the lowest spin concentrations accessible by the technique. Therefore, the 5-pulse DEER can alleviate two problems associated with the sensitivity of distance determination in membrane proteins labeled with nitroxide probes. Associated with the better signal to noise, and the possibility to detect longer distances with higher reliability, there come unfortunately artefacts in the time domain traces, which are due to partial excitation and excitation band overlap. However, the availability of AWG technology and recent developments in artefact correction methods [47,48] paved the way to the applicability of this new sequence to low concentrated membrane protein samples, where longer traces are needed to overcome the still challenging detection of long distances in membrane environments.

Even though the sensitivity and the reliability of the distance determination by DEER have tremendously improved, there are still challenges ahead which concern application in cellular context (even lower spin concentrations and presence of reducing agents), long distances (especially for membrane protein) and simultaneous reliable detection of a number of selective distances in multiprotein complexes when different spins are present. Studies of spin-labeled proteins or nucleic acids in cellular conditions are available (for example in [54,55]), but application to membrane proteins still faces severe challenges. Up to now, only one membrane protein in its native environment, namely BtuB in the outer membrane of *E. coli*, was studied using spectroscopically different labels [13,14]. Several limitations exist if one wants to address conformational changes of membrane proteins in the cell interior. Therefore, new biochemical methods and technical developments are required.

As mentioned before, to overcome the limitations intrinsic in complex spin systems and to optimize the distance detection, one can use other types of labels, which are spectroscopically orthogonal to nitroxides (e.g. carbon-, metal- based) and single frequency methods alternative to DEER to extract distances between spin pairs. In the following, we will briefly introduce Gd^{III}, trityl and Cu^{II} labels, and address some key advantages/disadvantages of the single frequency methods.

To work in the presence of reducing agents, or to have labels spectroscopically orthogonal to nitroxides, Gd^{III} labels are the most common alternative labels for proteins. The Q-band DEER setup with hard pulses still provides reliable Gd-Gd distance extraction, although, due to the large zero field splitting of the S = 7/2, the Q-band spectra are very broad, therefore only a relative small spin packets can be excited by conventional rectangular pulses. This implies that the modulation depth of the Gd-Gd DEER signal is extremely low. High power W-band setups with bimodal cavities demonstrated a superior sensitivity for Gd-based labels [9]. AWG-based prepolarization pulses and larger excitations in combination with high field, are the best choice to enhance the modulation depth of the DEER signals (for examples see [49–51]). Gd^{III} labels are in general larger than nitroxides, but the narrower spectral features, the absence of orientation selection artefacts at high fields and the possibility to use them under cellular conditions [52] make them good candidates for the future investigation of membrane proteins. The combination of nitroxide and gadolinium labels for orthogonal distance determination by DEER was demonstrated in 2012 [15,53] and it is nowadays an attractive possibility to study protein complexes and protein-protein interactions simultaneously. As an example, a bacterial ABC importer was labeled with two nitroxide probes and its substrate binding protein with one Gd^{III} probe. This strategy helped measuring simultaneously the nitroxide-nitroxide distances monitoring the movement of the transporter and the Gd-nitroxide distance between the transporter and its substrate binding protein during the nucleotide cycle [12].

Trityl radicals can be functionalized to be attached to protein sites [10], and provide a third option besides nitroxides and Gd-based labels. They are resistant to reducing agents, they have long relaxation times and a narrow spectral width. One can perform DEER to obtain trityl-trityl distances, but also use them in combination with nitroxide probes [54]. In the second case, the narrow spectral width of the trityl radicals allows a complete excitation, which increases the modulation depth of DEER traces when nitroxides are used as observer spins. Another advantage is that the long relaxation of trityl radicals may offer the possibility to use them as reporters of distances at physiological temperatures [55]. Notably, this opportunity is also explored for long relaxing nitroxide radicals which are sterically shielded [56].

Introducing copper ions in proteins via histidine binding sites is another alternative strategy to nitroxide labeling [57] and can be applied if functional cysteines are present. Both Cu-Cu distances and Cu-nitroxide distances can be obtained reliably. The large *g* anisotropy of copper induces possible orientation selection artefacts, which can be compensated by detection of few DEER traces at different magnetic fields [11].

Development of new labels also pushed alternative dipolar spectroscopy strategies, namely single frequency methods, which are briefly addressed in the following. Double Quantum Coherence (DQC) has the advantage of a better signal to noise ratio than DEER but suffers from background correction artefacts (see for example [58]). Relaxation Induced Dipolar Modulation Enhancement (RIDME) can be preferred over DEER if a fast relaxing species is present together with a slower relaxing one (e.g. low spin Fe^{3+}-nitroxide [59]), although the traces may have background decays difficult to correct. In this single frequency experiment, instead of actively flipping the second spin with a pulse (as in DEER), one of the spins has to flip by spontaneous relaxation during the time interval of the sequence, while the spin magnetization to be detected is stored along the magnetic field direction. Distance distributions between two high-spin paramagnetic centers can also be obtained via RIDME with higher sensitivity than in DEER. The traces are in this case affected by the presence of overtones of dipolar frequencies, which can be taken into account in data analysis to obtain reliable distance distributions (e.g. Gd-Gd [60]). The increasing interest on metal-based spins has also reactivated the use of other techniques such as the "2 + 1" [61] and the SIFTER (SIngle-Frequency TEchniques for Refocusing dipolar couplings) [62].

As described above, SDSL EPR can provide "only" site-directed information, and the "site" coincides with the location of the electron spin. For a nitroxide, this corresponds to the midpoint of the N-O bond, which is located at distance of about 0.8 nm from the protein backbone atoms through a linker characterized by rotatable bonds (five in case of MTSL, Fig. 1A) [24]. With the exception of the Cu^{II} ion bound to engineered histidine residues, the other available spin labels (e.g. trityl and Gd^{III}) are localized even further away from the backbone of the protein. Therefore, validating structural data or modeling protein conformational changes require simulations of the conformations adopted by the spin probe with respect to the protein backbone. This type of modeling is mostly done to support distance measurements and it makes use of coarse-grained approaches such as rotamer libraries of spin labels. Software packages are available such as MMM [24] and MtsslWizard [63], which allow to calculate *in silico* the populated rotamers of several probes attached to a protein site. If one PDB file is available for a protein in one state (e.g. from NMR, X-ray, etc.), one can predict the location of the spin-labeled side chain, and create coarse-grained models for proteins' structural changes. The number of EPR

constraints needed to decipher a molecular motion in a protein depends on the complexity of the motion, size of the proteins, quality of information needed and in general at least a few tens of distances must be detected for each protein.

5. Advantages and disadvantages of SDSL EPR with respect to other biophysical techniques

Although statistically underrepresented in the PDB due to intrinsic difficulties in sample preparation, protein yields, crystallization conditions, physiological membrane milieu, the available membrane protein structures were solved using three main techniques: X-ray crystallography, nuclear magnetic resonance (NMR) spectroscopy, and cryo electron-microscopy (EM) [64–67].

The following paragraphs briefly summarize how the distinctive features of SDSL EPR can be used in combination with other biophysical techniques to study structures and conformational changes of membrane proteins.

To obtain high resolution structures by X-ray crystallography, the selected membrane protein must form highly organized 3D crystals. Due to the organization in crystals, X-ray structures necessarily show a snapshot of a single protein state and provide only indications on dynamic regions in proteins. Maintaining the exact physiological membrane environment is a challenge in crystallography, because it would require to be able to crystallize the specific type of membrane bilayer associated with the protein.

When only one state of a membrane protein which undergoes conformational transitions is crystallized and one wants to explore its conformational transitions (e.g. nucleotide-induced changes, ligand-binding effects), or when the dynamic region of a protein needs to be investigated (e.g. loops, partially unfolded regions), a combination of X-ray with SDSL-EPR can be extremely useful (selected examples of monomeric and oligomeric membrane proteins can be found here [68–71]). Based on existing X-ray structures, preferred and accessible labeling sites can be identified, protein variants with one or two spin labels can be produced and the dynamics at each site together with interspin distances between two sites can be measured. Comparing the dynamics (mobility) of the singly-labeled variants under different experimental conditions or environments (e.g. apo-state against ligand bound state, detergent-solubilized against membrane-reconstituted) allows to monitor the properties of flexible regions of a protein and to study the effects of different triggers on the side chain dynamics. Detecting interspin distances of several pairs of labels in a membrane protein can add even more information on its conformational transitions. Notably, comparing data on membrane proteins in detergent and in membranes allows to validate existing structural models in more physiological environments, and to understand whether the protein captures the same fold in micelles, bicelles, nanodiscs and in membranes (see for example [12,72,73]). Additionally, with the help of modeling tools, it is possible to reconstruct the coarse-grained movements of the protein during its function. As case studies, we will show at the end of this review how we successfully used this combinatorial approach to unveil the structural changes of an apoptotic protein Bax upon membrane insertion [23], and to explore conformational equilibria in ABC transporters [38].

Besides conventional X-ray crystallography, femtosecond X-ray protein nanocrystallography became available in 2011 and was directly applied to photosystem I, one of the largest membrane protein ever crystallized [74]. Since then, structural biologists have exploited new opportunities to study membrane protein structure and dynamics using XFEL (X-ray Free Electron Laser) sources (see for example [75]). With XFEL it is possible to obtain structural data from micron or submicron scale crystals and to perform time-resolved studies of protein dynamics on an ultrafast time scale [76,77], which opens a very promising avenue for the characterization of conformational transitions of membrane proteins at atomic resolution.

Another X-ray related technique is SAXS (Small Angle X-ray Scattering), a low-resolution technique, mostly applied to soluble proteins (for a recent review see [78]). SAXS can be applied to systems with size and conformational polydispersity, including highly flexible objects. Applications on membrane proteins in detergent micelles are challenging because both the free detergent micelles and the “detergent belt” around the hydrophobic protein regions modify the scattering curves. However, it was shown that the combination of proper choice of detergents, size exclusion chromatography, SAXS, and refractometry can produce a complete structural model of a membrane protein in a detergent micelle [79].

In contrast to X-ray crystallography, NMR provides information about conformational dynamics under physiological conditions, thus rigid and flexible parts of a membrane protein can be recognized. Atomic resolution is achievable due to the large number of naturally occurring nuclear spins in the proteins. However, as in the EPR case, NMR samples also need to be isotopically labeled with different labeling schemes to reach a satisfying quality of the structural model. In general the amount of sample required for NMR is a factor 100 larger than for EPR. Moreover, the size of the proteins is limited to about 30 kDa in solution NMR and small membrane proteins can be only studied in detergent micelles or nanodiscs. Only solid state NMR allows to study larger membrane proteins under physiologically relevant conditions. The main challenge of NMR is the size of the protein, therefore full assignment of large membrane proteins and protein complexes remains a difficult task. SDSL EPR in combination with NMR can help building structural models (as seen for example in the case of a water soluble ribonucleoprotein [80]), by adding long range distance information, which are not available by NMR methods.

Cryo-EM is a method that can be applied to very large proteins and protein complexes at comparably low concentrations. After the “resolution revolution” [64,81], the cryo-EM resolution became comparable to that of X-ray crystallography. Still, there are some limitations for small protein sizes, flexible proteins or protein regions and non-unique protein oligomeric states (for example mixtures of monomer, dimers, and oligomers). In cryo-EM the images of many thousands of frozen particles are used to reconstruct the high-resolution model. Thereby, proteins in detergent micelles are preferred over membrane-embedded proteins, as the electron density of lipids and proteins is similar, making their assignment difficult. When large protein complexes are investigated, or when models of conformational changes are created, SDSL EPR distance measurements can be helpful in discriminating different models, or to aid the docking process adding additional constraints.

SDSL EPR can also be used to study protein-protein interactions at the membrane. Unveiling if two proteins interact or how many units constitute a homo-oligomer is a very easy task for EPR, given that each protein partner has one label. For a multi-protein interaction network, orthogonal labels could be used, e.g. Gd^{III}, Cu^{II}, nitroxide, etc. to disentangle the types of interactions among different proteins. Alternative methods are: Fluorescence Cross-Correlation Spectroscopy (FCCS) [82,83], Single Particle Tracking in Total Internal Reflection Fluorescence (SPT-TIRF) microscopy [82,84] and Förster Resonance Energy Transfer (FRET) experiments [85,86]. Those techniques have the main advantages that they require maximally nanomolar fluorophore concentrations, they can be used down to the single-molecule level and the probes can be genetically-encoded and therefore be used under *in vivo* conditions.

FCCS is a method with single particle sensitivity that can monitor the diffusion of the fluorophore through the focal volume of a confocal microscope. The scanning FCCS variant was developed to study membrane proteins *in vitro* and *in vivo* and it can be used to determine diffusion coefficients and protein-protein interactions. However, in contrast to SDSL EPR, FCCS cannot determine complex stoichiometry or distance information.

Diffusion coefficients, protein-protein interactions as well as

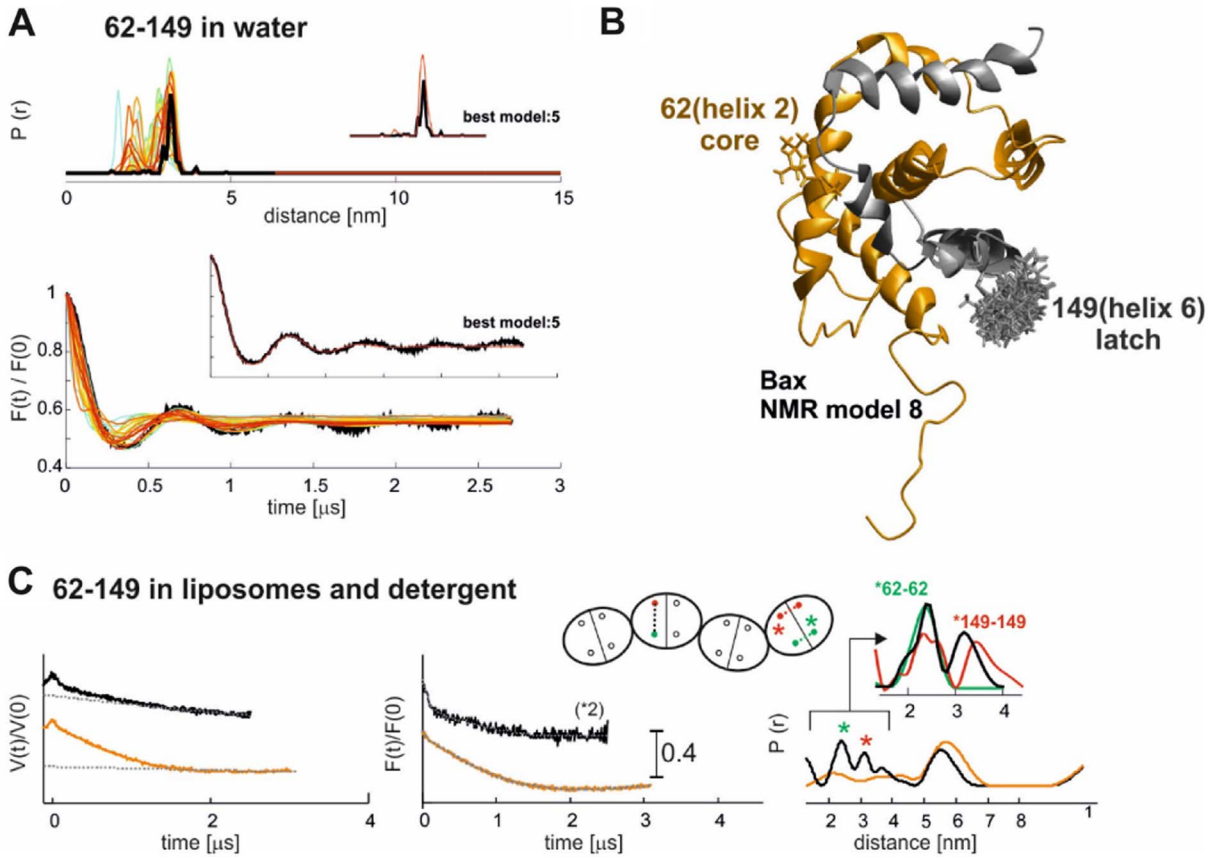

Fig. 4. Analysis of spin-labeled Bax in water and membrane environments. **A**) Experimental distance distribution between the MTSL attached at positions 62 and 149 (dark, upper panel) and background corrected DEER traces (dark, lower panel) superimposed to the simulated data on the 20 NMR models (colored, from PDB ID: 1F16). The insets show the simulation with the best root mean square deviation (NMR model number 5). **B**) In orange, the core domain of the monomeric Bax unit with the spin-labeled position 62; in black, the latch domain with the spin-labeled position 149. Only one MTSL rotamer is populated in this NMR model (number 8) for position 62, while several are populated for position 149. **C**) DEER data on the same pair when Bax (spin diluted) is embedded in membranes. The data are recorded in liposomes (black) and in detergent micelles (orange). Comparison of both traces reveal that the background is over-corrected in the trace obtained in liposomes due to the too short length of the dipolar evolution time, thus the long distance component is suppressed in the overall distribution. The short distances are shown to be the characteristic ones of the inter-monomer interactions between pairs of 62 labels (green asterisk) and pairs of 149 (red asterisk) in neighboring monomeric units. These residual components are expected from the 1:3 spin dilution method, see sketch of the spin-diluted oligomers, with dimeric building blocks. The inset shows the comparison of the distance distributions obtained with the respective singly-labeled mutants (red and green) to validate the assignment.

stoichiometries can be derived from SPT-TIRF microscopy experiments. In this single molecule technique, a few hundred or thousands of particles are analyzed one by one in each experiment, which makes it more time consuming than SDSL EPR. Moreover, SPT-TIRF needs evanescent waves and thus measurements are limited to areas close to the glass. Therefore, only immobilized systems like proteins in supported lipid bilayers or in plasma-membranes of immobilized cells can be studied, while proteins in organelles, isolated membranes or liposomes are not accessible to SPT-TIRF.

FRET and EPR dipolar spectroscopy deliver closely related information on inter-label distances in proteins. The main advantage of FRET relies on the fact that it can be applied to batch (nanomolar concentrations) and single molecule samples at physiological temperature, while EPR provides distance information on frozen molecular ensemble at micromolar concentrations. FRET uses the energy- transfer between a donor and an acceptor fluorophore attached at two sites, which are in general bulkier than the two identical MTSL bound to the corresponding positions and can induce problems in protein structure or function. For exact distance determination in FRET, the orientation between the donor and acceptor molecules must be known and this is difficult to achieve [87]. As stated above, in DEER it is possible to use non-selective pulse detection schemes which suppress the orientation selection for nitroxide probes, which is desirable for the analysis of spin-labeled membrane proteins [37]. Additionally, the nitroxide probes bound to sites in membrane proteins are not generally geometrically correlated, which additionally minimizes the orientation selectivity problem. However, at high fields one can also obtain the relative orientations of two rigid geometrically correlated nitroxide molecules (see for example [88]).

Moreover, each FRET pair has only a small distance window in which accurate distances information can be gained, and this implies that to monitor distance changes within a protein system in a wide range (e.g. 1–10 nm) one needs to use different FRET pairs. Finally, the fluorescent properties of fluorophores are often affected by the environments. Thus, when membrane proteins are studied, FRET results can be affected by the amount of lipids in contact with the fluorophore, which again complicates exact distance determination.

6. Applications in membrane proteins: I. Proapoptotic Bax

Bcl-2 proteins are key players in apoptosis, a form of programmed cell death crucial for all mammalian species [89]. Bcl-2 proteins are important targets in drug development as desensitization against apoptosis is a hallmark of cancer and increased apoptotic rates provoke severe diseases [90]. About 20 pro- and anti-apoptotic Bcl-2 protein family members are known and their interplay determines cell fate. Several family members have the rare capacity to switch between soluble and membrane-embedded conformations [91–93], with the latter being crucial for apoptosis. Structures of soluble Bcl-2 proteins were solved using NMR or X-ray techniques [94–96], while the active,

membrane-embedded conformations and the multi-protein complexes are still not well understood. EPR spectroscopy has proven to be a very powerful tool to study topology, structure, interactions and conformational changes of the Bcl-2 proteins Bax, BakΔC and Bid [23,91,97–99]. In healthy cells, all three proteins are monomeric, soluble and inactive [94,100]. Upon pro-apoptotic stimuli, Bid is cleaved by Caspase 8, creating the active form cBid [101,102], which can translocate to the mitochondrial outer membrane and activate Bax as well as its homologue Bak [103,104]. This provokes large conformational changes in Bax and Bak [23,105,106]: they insert deeply into the membrane, form homo-oligomers and induce stable pores in the membranes [107–109], which is in most cases the point of no return in cell death initiation [110].

To form pores, Bax undergoes a complex rearrangement from a water soluble, inactive and monomeric form to a membrane-bound, oligomeric form, which can be studied via EPR techniques. By detecting a series of CW EPR spectra at regular time intervals (e.g. each minute), we could follow the kinetics of the membrane insertion process by monitoring the changes in mobility of Bax wildtype labeled at the two natural cysteines (Fig. 2A) [99], and the influence of different factors such as membrane composition and concentration of the proapoptotic activator cBid [99].

Additionally, we studied Bax conformational changes from the water soluble to the membrane-embedded state via interspin distance determination using > 40 singly and doubly spin labeled variants [23]. Analyzing the interspin distances obtained in the water soluble form of Bax, we found a root mean square deviation as small as 0.3 nm [23] between the measured distances (in the frozen state) and those simulated based on the NMR structure. This is in line with the expected errors using the rotamer library approach [111] and it proves that freezing does not perturb the structure of this globular protein. The experimental DEER constraints were successfully used to model the structure of Bax by a *de-novo* approach [112], demonstrating the reliability of the mean distances extracted from the analysis of the water-soluble protein.

In Fig. 4A an example of a 4p-DEER trace detected on the water soluble Bax spin labeled at positions 62 and 149 is shown (black) with the simulated distances performed on the 20 NMR models (colored). This pair has a sharp distance distribution (0.5 nm full width at half maximum) centered at 3.2 nm, due to the restricted space available for the spin label at position 62 (few rotamers simulated, see Fig. 4B). Narrow distance distributions produce persistent dipolar oscillations in the DEER trace (Fig. 4A), therefore background correction and data analysis are straightforward, and the distributions are extremely reliable. However, as in this case, slight variations in the NMR structures lead to distinct changes of the simulated distance distributions (the 3 nm distance peak is accompanied by a 2 nm distance peak in some models), highlighting the role of the neighboring amino acids in determining the experimental and simulated distance distributions. From this it follows that exposed residues with minor steric restrictions, therefore broader distance distributions, are preferred for reliable distance determination and modeling.

The data detection and processing was more complicated for the membrane-embedded Bax homo-oligomers. Those are built by multimers of dimers [99,113], so that when singly labeled monomers are used, both intra- and inter-dimer distances are detectable and their assignment is difficult. In this case, the non-homogeneous size distribution of the oligomers poses even more severe challenges in EPR, which add up to the lower sensitivity introduced by the lipid environment (see Fig. 3). For doubly labeled Bax variants, the situation is even more complicated due to the presence of four spins within a dimer. In this case, we tried to highlight only the intra-monomer distances in the active membrane-embedded state by using spin dilution, namely incubating doubly spin labeled and unlabeled Bax in a 1:3 ratio. This is a good compromise to statistically minimize the inter-monomer contribution to the distribution of distances detected without impairing too much the detection sensitivity.

Our results showed that there are two regions in the dimeric unit. The “core” or “dimerization” domain, which is structurally stable and forms a dimer of helices 2–5, and the “latch” or “piercing” domain (helices 6–9), which is important for pore formation and has some flexible hinges allowing conformational dynamic. The dynamic nature of this region makes its structural characterization difficult, and only EPR, accessibility and cross link experiments were so far able to give some structural insights [23,98,106,114,115]. To further complicate the analysis, helices 6–9 form also dimer-dimer contacts [23,114,116]. Therefore, most DEER distances between the core and latch domains were broadly distributed and centered at around 5–6 nm (see example in Fig. 4C). To reliably characterize such large distributions of rather long distances in membrane-embedded proteins one would need to detect dipolar time traces longer than 5–6 μs, with good signal-to-noise ratio, which was not possible with these samples using 4p-DEER (5p-DEER could be an option to improve data reliability). Therefore, we complemented the data in liposomes with data obtained with detergent micelles, and made use of available distance information obtained with singly-labeled variants to disentangle the different residual distance contributions (Fig. 4). Only with this detailed analysis we could extract reliable mean distances to be used for coarse-grained modeling of Bax embedded in the membrane. Based on several distance constraints per chosen spin-labeled site, we could validate the existing X-ray structure of the core dimeric region [23,105], as well as to suggest the first low resolution model of membrane-embedded Bax (using a multilateration process) [23]. This example clearly demonstrates that flexible regions of membrane proteins, which are notoriously difficult to characterize, can be recognized with CW EPR at physiological temperature (mobility of the spin labels), and the extent of their disorder can be measured by DEER at cryo temperatures even in large oligomers.

7. Applications in membrane proteins: II. Conformational equilibria of a heterodimeric ABC exporter

ABC exporters pump substrates across the membrane by coupling ATP-driven movements of nucleotide binding domains (NBDs) to the transmembrane domains (TMDs), which switch between inward- and outward-facing orientations. Site-directed spin labeling has been successfully applied to both importers and exporters, providing insight into the protein conformational steps necessary for substrate translocation. Three selected examples of such studies on bacterial ABC importers such as the maltose and the vitamin B_{12} importers from *E. coli* and the energy coupling factor from *L. lactis* can be found here [12,117,118].

The subgroup of ABC exporters, which we want to describe here in more detail, was extensively studied by EPR. The homodimeric lipid A exporter MsbA was fully characterized in terms of changes in the water accessibility and interspin distances during the nucleotide cycle [72,119–123]. The inward- to outward- facing transition was found to be induced in this homodimeric exporter by trapping the transition state intermediate with vanadate as well as by the ATP analogue AMP-PNP; the cofactor Mg^{2+} was recognized to be an important factor to ensure a complete switch to the OF conformation. Replacement of Mg^{2+} with the paramagnetic analogue Mn^{2+} (spin 5/2) introduces two paramagnetic metal ion centers in the nucleotide binding sites, which can be in principle be used as additional probes orthogonal to the nitroxides for distance measurements [124], as well as to directly detect ATP turnover via hyperfine spectroscopy [125].

EPR methods were used recently to unveil the structural role of the asymmetries found in the two nucleotide binding sites of a bacterial heterodimeric exporter from *T. maritima* [38] and of the human Pgp [68] (also known as ABCB1, single polypeptide chain). The detailed study of the conformational transition during substrate translocation and of the structural relevance of the asymmetries in exporters is relevant because Pgp is responsible for the clearance of xenobiotics and in cancer resistance to chemotherapy. The bacterial analogues offer the

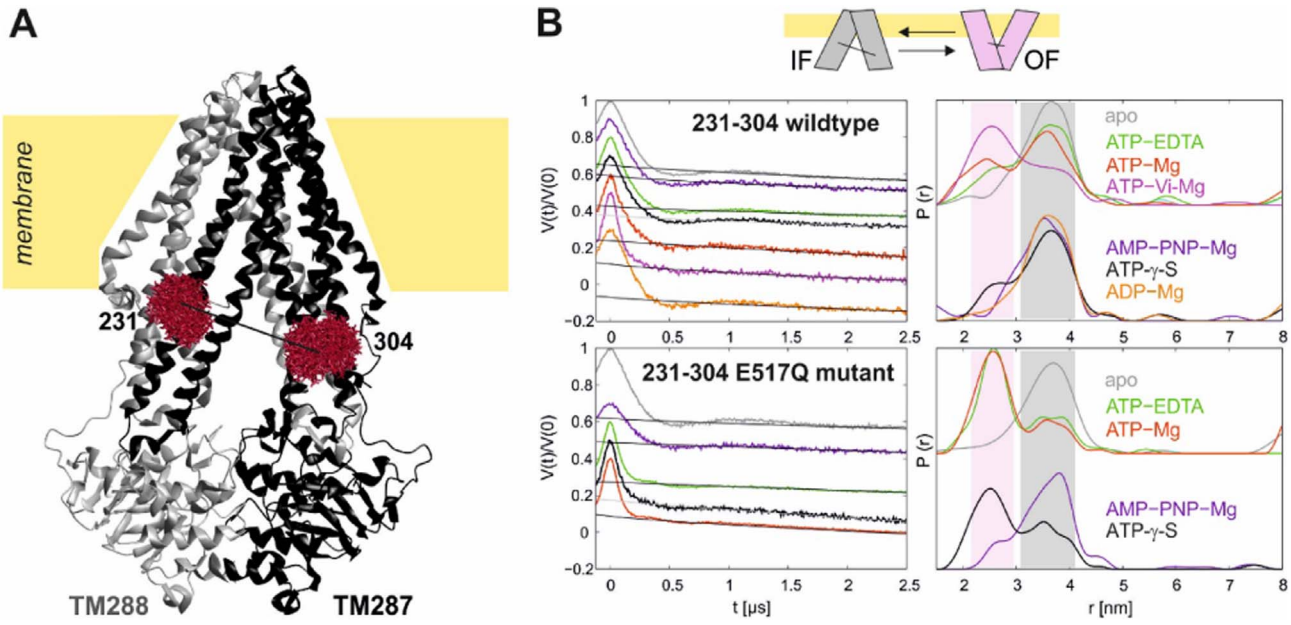

Fig. 5. Conformational equilibria in the ABC exporter TM287/288. **A**) Structure of the TM287/288 transporter in its apo state (PDB ID: 4Q4H). The two spin-labeled intracellular positions in the subunit TM287 are highlighted in red. **B**) A sketch of the IF to OF transition is shown, highlighting the expected decrease in interspin distance in the intracellular region of the transporter. The upper panel shows the primary DEER data obtained in spin-labeled transporters (wildtype background) solubilized in detergent micelles upon incubation with different nucleotides listed in the figure legend. ATP-Vi-Mg represents the transition state intermediate trapped with vanadate; AMP-PNP and ATP-γ-S are two ATP analogues. The bottom panel shows the same type of data detected on the E517Q mutant variant, which has a strongly impaired ATP hydrolysis. The grey and pink rectangles highlight the 3.5 nm distance (corresponding to the IF state) and the 2.5 nm distance (OF state).

advantage that they can be produced with higher yield allowing to elucidate the intriguing characteristic features of this asymmetric version of ABC exporters. Notably, a bacterial heterodimeric exporter was proven to be a fully functional analogue of the mammalian antigen transporter TAP [126], which confirms the shared key mechanistic properties among the members of this subfamily.

Here we describe the use of DEER to elucidate the conformational transitions in the heterodimeric ABC exporter TM287/288 from the hyperthermophile *T. maritima,* which contains a non-canonical ATP binding site (so called degenerate site), in which ATP hydrolysis is impaired (Fig. 5). The EPR study was performed with six pairs of spin-labeled sites located in the nucleotide binding domains (NBDs), in the intracellular region, and in the extracellular region of the transporter to map its movement in response of a variety of nucleotides and nucleotide analogues.

Fig. 5 shows DEER data obtained for the intracellular pair 231–304, which has a characteristic distance of 3.5 nm when the transporter is in its apo form (grey in Fig. 5B). A second distance of 2.5 nm, indicative of a closed intracellular region expected for an outward-facing (OF) state of the transporter is populated in the presence of nucleotides. If a transition state intermediate was trapped with vanadate ions (magenta in Fig. 5B) we obtained the highest fraction of OF states in the molecular ensemble. With other nucleotides the equilibrium is more shifted towards the inward-facing (IF) state, as shown clearly by the EPR snapshots at cryo temperatures with distinct distance peaks at both 2.5 and 3.5 nm (Fig. 5B). In contrast to the homodimeric transporters, the ATP analogue AMP-PNP is found to be insufficient to close the asymmetric NBDS and to induce the transition to the OF state. This seems to be a common feature in asymmetric transporters, as it was confirmed in Pgp as well [126]. However, while in Pgp the OF state could only be populated in the post hydrolytic state trapped by vanadate, in TM287/288 ATP binding without hydrolysis was sufficient to partially populate the OF state. Using a single point mutation as E517Q in the subunit 287, we observed a shift in the conformational equilibria with respect to the wildtype background (Fig. 5B, upper vs lower panel), and we concluded that a full switch to the OF state is also induced if nucleotides were trapped in a pre-hydrolytic state.

Concluding, by using EPR we could show that a molecular feature differentiating heterodimeric ABC exporters from their homodimeric counterparts is that they exist in conformational equilibrium between the IF and OF states. The thermodynamic details of the discovered equilibrium seem to be species specific. How the substrate is altering this equilibrium, how the translocation events take place and why the stimulatory effect of drugs turns into inhibitory ones at high concentrations are the next challenges ahead, which can be addressed by EPR methods.

Transparency document

The Transparency document associated with this article can be found, in online version.

Acknowledgments

We would like to thank M. Teucher for the help in preparation of Fig. 2 and M. Hadi Timachi for Fig. 3; M. Teucher and L. Galazzo for proof reading of the manuscript. This work is supported by the DFG Cluster of Excellence RESOLV (EXC 1069) funded by the Deutsche Forschungsgemeinschaft.

References

[1] J. Zimmerberg, K. Gawrisch, The physical chemistry of biological membranes, Nat. Chem. Biol. 2 (2006) 564–567.
[2] S.H. White, Biophysical dissection of membrane proteins, Nature 459 (2009) 344–346.
[3] C. Altenbach, T. Marti, H. Khorana, W. Hubbell, Transmembrane protein structure: spin labeling of bacteriorhodopsin mutants, Science 248 (1990) 1088–1092.
[4] E. Bordignon, Y. Polyhach, EPR techniques to probe insertion and conformation of spin-labeled proteins in lipid bilayers, Methods Mol. Biol. 974 (2013) 329–355.
[5] M.R. Fleissner, E.M. Brustad, T. Kálai, C. Altenbach, D. Cascio, F.B. Peters, K. Hideg, S. Peuker, P.G. Schultz, W.L. Hubbell, Site-directed spin labeling of a genetically encoded unnatural amino acid, Proc. Natl. Acad. Sci. U. S. A. 106 (2009) 21637–21642.
[6] M.J. Schmidt, A. Fedoseev, D. Summerer, M. Drescher, Genetically encoded spin labels for in vitro and in-cell EPR studies of native proteins, Methods Enzymol. 563

(2015) 483–502.
[7] M. Lorenzi, C. Puppo, R. Lebrun, S. Lignon, V. Roubaud, M. Martinho, E. Mileo, P. Tordo, S.R.A. Marque, B. Gontero, B. Guigliarelli, V. Belle, Tyrosine-targeted spin labeling and EPR spectroscopy: an alternative strategy for studying structural transitions in proteins, Angew. Chem. Int. Ed. 50 (2011) 9108–9111.
[8] E. Bordignon, EPR spectroscopy of nitroxide spin probes, eMagRes 6 (2) (2017) 235–254.
[9] A. Feintuch, G. Otting, D. Goldfarb, Gd3 + spin labeling for measuring distances in biomacromolecules, Methods Enzymol. 563 (2015) 415–457.
[10] J.J. Jassoy, A. Berndhäuser, F. Duthie, S.P. Kühn, G. Hagelueken, O. Schiemann, Versatile trityl spin labels for nanometer distance measurements on biomolecules in vitro and within cells, Angew. Chem. Int. Ed. 56 (2017) 177–181.
[11] Z. Yang, M. Ji, T.F. Cunningham, S. Saxena, Cu2 + as an ESR probe of protein structure and function, Methods Enzymol. 563 (2015) 459–481.
[12] B. Joseph, V.M. Korkhov, M. Yulikov, G. Jeschke, E. Bordignon, Conformational cycle of the vitamin B12 ABC importer in liposomes detected by double electron-electron resonance (DEER), J. Biol. Chem. 289 (2014) 3176–3185.
[13] B. Joseph, A. Sikora, E. Bordignon, G. Jeschke, D.S. Cafiso, T.F. Prisner, Distance measurement on an endogenous membrane transporter in *E. coli* cells and native membranes using EPR spectroscopy, Angew. Chem. Int. Ed. 54 (2015) 6196–6199.
[14] B. Joseph, V.M. Tormyshev, O.Y. Rogozhnikova, D. Akhmetzyanov, E.G. Bagryanskaya, T.F. Prisner, Selective high-resolution detection of membrane protein–ligand interaction in native membranes using trityl–nitroxide PELDOR, Angew. Chem. Int. Ed. 55 (2016) 11538–11542.
[15] P. Lueders, H. Jäger, M.A. Hemminga, G. Jeschke, M. Yulikov, Distance measurements on orthogonally spin-labeled membrane spanning WALP23 polypeptides, J. Phys. Chem. B 117 (2013) 2061–2068.
[16] S. Stoll, A. Schweiger, EasySpin, a comprehensive software package for spectral simulation and analysis in EPR, J. Magn. Reson. 178 (2006) 42–55.
[17] Z. Zhang, M.R. Fleissner, D.S. Tipikin, Z. Liang, J.K. Moscicki, K.A. Earle, W.L. Hubbell, J.H. Freed, Multifrequency electron spin resonance study of the dynamics of spin labeled T4 lysozyme, J. Phys. Chem. B 114 (2010) 5503–5521.
[18] E. Bordignon, J.P. Klare, M. Doebber, A.A. Wegener, S. Martell, M. Engelhard, H.-J. Steinhoff, Structural analysis of a HAMP domain: the linker region of the transducer in complex with sensory rhodopsin II, J. Biol. Chem. 280 (2005) 38767–38775.
[19] D.G. Mitchell, R.W. Quine, M. Tseitlin, S.S. Eaton, G.R. Eaton, X-band rapid-scan EPR of nitroxyl radicals, J. Magn. Reson. 214 (2012) 221–226.
[20] S.S. Eaton, G.R. Eaton, Rapid-scan EPR of nitroxide spin labels and semiquinones, Methods Enzymol. 563 (2015) 3–21.
[21] J.R. Biller, D.G. Mitchell, M. Tseytlin, H. Elajaili, G.A. Rinard, R.W. Quine, S.S. Eaton, G.R. Eaton, Rapid scan electron paramagnetic resonance opens new avenues for imaging physiologically important parameters in vivo, J. Vis. Exp. 115 (2016) 54068.
[22] E. Bordignon, H.-J. Steinhoff, Membrane Protein Structure and Dynamics Studied by Site-Directed Spin-Labeling ESR, ESR Spectroscopy in Membrane Biophysics, Springer, US, 2007, pp. 129–164.
[23] S. Bleicken, G. Jeschke, C. Stegmueller, R. Salvador-Gallego, Ana J. García-Sáez, E. Bordignon, Structural model of active Bax at the membrane, Mol. Cell 56 (2014) 496–505.
[24] Y. Polyhach, E. Bordignon, G. Jeschke, Rotamer libraries of spin labelled cysteines for protein studies, Phys. Chem. Chem. Phys. 13 (2011) 2356–2366.
[25] A. Doll, E. Bordignon, B. Joseph, R. Tschaggelar, G. Jeschke, Liquid state DNP for water accessibility measurements on spin-labeled membrane proteins at physiological temperatures, J. Magn. Reson. 222 (2012) 34–43.
[26] R. Carmieli, N. Papo, H. Zimmermann, A. Potapov, Y. Shai, D. Goldfarb, Utilizing ESEEM spectroscopy to locate the position of specific regions of membrane-active peptides within model membranes, Biophys. J. 90 (2006) 492–505.
[27] A. Volkov, C. Dockter, T. Bund, H. Paulsen, G. Jeschke, Pulsed EPR determination of water accessibility to spin-labeled amino acid residues in LHCIIb, Biophys. J. 96 (2009) 1124–1141.
[28] E. Matalon, I. Kaminker, H. Zimmermann, M. Eisenstein, Y. Shai, D. Goldfarb, Topology of the trans-membrane peptide WALP23 in model membranes under negative mismatch conditions, J. Phys. Chem. B 117 (2013) 2280–2293.
[29] E. Bordignon, A.I. Nalepa, A. Savitsky, L. Braun, G. Jeschke, Changes in the microenvironment of nitroxide radicals around the glass transition temperature, J. Phys. Chem. B 119 (2015) 13797–13806.
[30] I. Kaminker, R. Barnes, S. Han, Overhauser dynamic nuclear polarization studies on local water dynamics, Methods Enzymol. 564 (2015) 457–483.
[31] O. Fisette, C. Päslack, R. Barnes, J.M. Isas, R. Langen, M. Heyden, S. Han, L.V. Schäfer, Hydration dynamics of a peripheral membrane protein, J. Am. Chem. Soc. 138 (2016) 11526–11535.
[32] T.F. Segawa, M. Doppelbauer, L. Garbuio, A. Doll, Y.O. Polyhach, G. Jeschke, Water accessibility in a membrane-inserting peptide comparing overhauser DNP and pulse EPR methods, J. Chem. Phys. 144 (2016) 194201.
[33] J.E. Banham, C.M. Baker, S. Ceola, I.J. Day, G.H. Grant, E.J.J. Groenen, C.T. Rodgers, G. Jeschke, C.R. Timmel, Distance measurements in the borderline region of applicability of CW EPR and DEER: a model study on a homologous series of spin-labelled peptides, J. Magn. Reson. 191 (2008) 202–218.
[34] M. Pannier, S. Veit, A. Godt, G. Jeschke, H.W. Spiess, Dead-time free measurement of dipole–dipole interactions between electron spins, J. Magn. Reson. 142 (2000) 331–340.
[35] G. Jeschke, V. Chechik, P. Ionita, A. Godt, H. Zimmermann, J. Banham, C.R. Timmel, D. Hilger, H. Jung, DeerAnalysis2006—a comprehensive software package for analyzing pulsed ELDOR data, Appl. Magn. Reson. 30 (2006) 473–498.
[36] T. Schmidt, M.A. Wälti, J.L. Baber, E.J. Hustedt, G.M. Clore, Long distance measurements up to 160 Å in the GroEL tetradecamer using Q-band DEER EPR spectroscopy, Angew. Chem. Int. Ed. 128 (2016) 16137–16141.
[37] Y. Polyhach, E. Bordignon, R. Tschaggelar, S. Gandra, A. Godt, G. Jeschke, High sensitivity and versatility of the DEER experiment on nitroxide radical pairs at Q-band frequencies, Phys. Chem. Chem. Phys. 14 (2012) 10762–10773.
[38] M.H. Timachi, C.A. Hutter, M. Hohl, T. Assafa, S. Bohm, A. Mittal, M.A. Seeger, E. Bordignon, Exploring conformational equilibria of a heterodimeric ABC transporter, elife 6 (2017).
[39] T. von Hagens, Y. Polyhach, M. Sajid, A. Godt, G. Jeschke, Suppression of ghost distances in multiple-spin double electron-electron resonance, Phys. Chem. Chem. Phys. 15 (2013) 5854–5866.
[40] A. Giannoulis, R. Ward, E. Branigan, J.H. Naismith, B.E. Bode, PELDOR in rotationally symmetric homo-oligomers, Mol. Phys. 111 (2013) 2845–2854.
[41] H. Celia, N. Noinaj, S.D. Zakharov, E. Bordignon, I. Botos, M. Santamaria, T.J. Barnard, W.A. Cramer, R. Lloubes, S.K. Buchanan, Structural insight into the role of the Ton complex in energy transduction, Nature 538 (2016) 60–65.
[42] G. Hagelueken, W.J. Ingledew, H. Huang, B. Petrovic-Stojanovska, C. Whitfield, H. ElMkami, O. Schiemann, J.H. Naismith, PELDOR distance fingerprinting of the octameric outer-membrane protein Wza from *Escherichia coli*, Angew. Chem. Int. Ed. 48 (2009) 2904–2906.
[43] P.E. Spindler, P. Schöps, W. Kallies, S.J. Glaser, T.F. Prisner, Perspectives of shaped pulses for EPR spectroscopy, J. Magn. Reson. 280 (2017) 30–45.
[44] A. Doll, G. Jeschke, Wideband frequency-swept excitation in pulsed EPR spectroscopy, J. Magn. Reson. 280 (2017) 46–62.
[45] P.E. Spindler, P. Schöps, A.M. Bowen, B. Endeward, T.F. Prisner, Shaped pulses in EPR, eMagRes 5 (4) (2016) 1477–1492.
[46] P.P. Borbat, E.R. Georgieva, J.H. Freed, Improved sensitivity for long-distance measurements in biomolecules: five-pulse double electron–electron resonance, J. Phys. Chem. Lett. 4 (2013) 170–175.
[47] F.D. Breitgoff, J. Soetbeer, A. Doll, G. Jeschke, Y.O. Polyhach, Artefact suppression in 5-pulse double electron electron resonance for distance distribution measurements, Phys. Chem. Chem. Phys. 19 (2017) 15766–15779.
[48] F.D. Breitgoff, Y.O. Polyhach, G. Jeschke, Reliable nanometre-range distance distributions from 5-pulse double electron electron resonance, Phys. Chem. Chem. Phys. 19 (2017) 15754–15765.
[49] A. Doll, M. Qi, S. Pribitzer, N. Wili, M. Yulikov, A. Godt, G. Jeschke, Sensitivity enhancement by population transfer in Gd(iii) spin labels, Phys. Chem. Chem. Phys. 17 (2015) 7334–7344.
[50] A. Doll, M. Qi, N. Wili, S. Pribitzer, A. Godt, G. Jeschke, Gd(III)–Gd(III) distance measurements with chirp pump pulses, J. Magn. Reson. 259 (2015) 153–162.
[51] T. Bahrenberg, Y. Rosenski, R. Carmieli, K. Zibzener, M. Qi, V. Frydman, A. Godt, D. Goldfarb, A. Feintuch, Improved sensitivity for W-band Gd(III)-Gd(III) and nitroxide-nitroxide DEER measurements with shaped pulses, J. Magn. Reson. 283 (2017) 1–13.
[52] Y. Yang, F. Yang, Y.J. Gong, J.L. Chen, D. Goldfarb, X.C. Su, A reactive, rigid GdIII labeling tag for in-cell EPR distance measurements in proteins, Angew. Chem. Int. Ed. 56 (2017) 2914–2918.
[53] I. Kaminker, H. Yagi, T. Huber, A. Feintuch, G. Otting, D. Goldfarb, Spectroscopic selection of distance measurements in a protein dimer with mixed nitroxide and Gd3 + spin labels, Phys. Chem. Chem. Phys. 14 (2012) 4355–4358.
[54] G.Y. Shevelev, O.A. Krumkacheva, A.A. Lomzov, A.A. Kuzhelev, D.V. Trukhin, O.Y. Rogozhnikova, V.M. Tormyshev, D.V. Pyshnyi, M.V. Fedin, E.G. Bagryanskaya, Triarylmethyl labels: toward improving the accuracy of EPR nanoscale distance measurements in DNAs, J. Phys. Chem. B 119 (2015) 13641–13648.
[55] O. Krumkacheva, E. Bagryanskaya, EPR-based distance measurements at ambient temperature, J. Magn. Reson. 280 (2017) 117–126.
[56] V. Meyer, Michael A. Swanson, Laura J. Clouston, Przemysław J. Boratyński, Richard A. Stein, Hassane S. McHaourab, A. Rajca, Sandra S. Eaton, Gareth R. Eaton, Room-temperature distance measurements of immobilized spin-labeled protein by DEER/PELDOR, Biophys. J. 108 (2015) 1213–1219.
[57] T.F. Cunningham, M.R. Putterman, A. Desai, W.S. Horne, S. Saxena, The double-histidine Cu(2 +)-binding motif: a highly rigid, site-specific spin probe for electron spin resonance distance measurements, Angew. Chem. Int. Ed. 54 (2015) 6330–6334.
[58] P.P. Borbat, H.S. McHaourab, J.H. Freed, Protein structure determination using long-distance constraints from double-quantum coherence ESR: study of T4 lysozyme, J. Am. Chem. Soc. 124 (2002) 5304–5314.
[59] D. Abdullin, F. Duthie, A. Meyer, E.S. Müller, G. Hagelueken, O. Schiemann, Comparison of PELDOR and RIDME for distance measurements between nitroxides and low-spin Fe(III) ions, J. Phys. Chem. B 119 (2015) 13534–13542.
[60] K. Keller, V. Mertens, M. Qi, A.I. Nalepa, A. Godt, A. Savitsky, G. Jeschke, M. Yulikov, Computing distance distributions from dipolar evolution data with overtones: RIDME spectroscopy with Gd(iii)-based spin labels, Phys. Chem. Chem. Phys. 19 (2017) 17856–17876.
[61] V.V. Kurshev, A.M. Raitsimring, Y.D. Tsvetkov, Selection of dipolar interaction by the “2 + 1” pulse train ESE, J. Magn. Reson. 81 (1989) (1969) 441–454.
[62] G. Jeschke, M. Pannier, A. Godt, H.W. Spiess, Dipolar spectroscopy and spin alignment in electron paramagnetic resonance, Chem. Phys. Lett. 331 (2000) 243–252.
[63] G. Hagelueken, D. Abdullin, O. Schiemann, mtsslSuite, Methods Enzymol. 563 (2015) 595–622.
[64] W. Kühlbrandt, Cryo-EM enters a new era, elife 3 (2014) e03678.
[65] P.R.L. Markwick, T. Malliavin, M. Nilges, Structural biology by NMR: structure, dynamics, and interactions, PLoS Comput. Biol. 4 (2008) e1000168.

[66] M. Billeter, G. Wagner, K. Wuthrich, Solution NMR structure determination of proteins revisited, J. Biomol. NMR 42 (2008) 155–158.
[67] I.D. Campbell, The march of structural biology, Nat. Rev. Mol. Cell Biol. 3 (2002) 377–381.
[68] B. Verhalen, R. Dastvan, S. Thangapandian, Y. Peskova, H.A. Koteiche, R.K. Nakamoto, E. Tajkhorshid, H.S. McHaourab, Energy transduction and alternating access of the mammalian ABC transporter P-glycoprotein, Nature 543 (2017) 738–741.
[69] C. Arrigoni, A. Rohaim, D. Shaya, F. Findeisen, R.A. Stein, S.R. Nurva, S. Mishra, H.S. McHaourab, D.L. Minor, Unfolding of a temperature-sensitive domain controls voltage-gated channel activation, Cell 164 (2016) 922–936.
[70] C. Pliotas, R. Ward, E. Branigan, A. Rasmussen, G. Hagelueken, H. Huang, S.S. Black, I.R. Booth, O. Schiemann, J.H. Naismith, Conformational state of the MscS mechanosensitive channel in solution revealed by pulsed electron–electron double resonance (PELDOR) spectroscopy, Proc. Natl. Acad. Sci. U. S. A. 109 (2012) E2675–E2682.
[71] N. Van Eps, L.N. Caro, T. Morizumi, A.K. Kusnetzow, M. Szczepek, K.P. Hofmann, T.H. Bayburt, S.G. Sligar, O.P. Ernst, W.L. Hubbell, Conformational equilibria of light-activated rhodopsin in nanodiscs, Proc. Natl. Acad. Sci. U. S. A. 114 (2017) E3268–E3275.
[72] P. Zou, M. Bortolus, H.S. McHaourab, Conformational cycle of the ABC transporter MsbA in liposomes: detailed analysis using double electron-electron resonance spectroscopy, J. Mol. Biol. 393 (2009) 586–597.
[73] R. Ward, C. Pliotas, E. Branigan, C. Hacker, A. Rasmussen, G. Hagelueken, Ian R. Booth, S. Miller, J. Lucocq, James H. Naismith, O. Schiemann, Probing the structure of the mechanosensitive channel of small conductance in lipid bilayers with pulsed electron-electron double resonance, Biophys. J. 106 (2014) 834–842.
[74] H.N. Chapman, P. Fromme, A. Barty, T.A. White, R.A. Kirian, A. Aquila, M.S. Hunter, J. Schulz, D.P. DePonte, U. Weierstall, R.B. Doak, F.R.N.C. Maia, A.V. Martin, I. Schlichting, L. Lomb, N. Coppola, R.L. Shoeman, S.W. Epp, R. Hartmann, D. Rolles, A. Rudenko, L. Foucar, N. Kimmel, G. Weidenspointner, P. Holl, M. Liang, M. Barthelmess, C. Caleman, S. Boutet, M.J. Bogan, J. Krzywinski, C. Bostedt, S. Bajt, L. Gumprecht, B. Rudek, B. Erk, C. Schmidt, A. Hömke, C. Reich, D. Pietschner, L. Strüder, G. Hauser, H. Gorke, J. Ullrich, S. Herrmann, G. Schaller, F. Schopper, H. Soltau, K.-U. Kühnel, M. Messerschmidt, J.D. Bozek, S.P. Hau-Riege, M. Frank, C.Y. Hampton, R.G. Sierra, D. Starodub, G.J. Williams, J. Hajdu, N. Timneanu, M.M. Seibert, J. Andreasson, A. Rocker, O. Jönsson, M. Svenda, S. Stern, K. Nass, R. Andritschke, C.-D. Schröter, F. Krasniqi, M. Bott, K.E. Schmidt, X. Wang, I. Grotjohann, J.M. Holton, T.R.M. Barends, R. Neutze, S. Marchesini, R. Fromme, S. Schorb, D. Rupp, M. Adolph, T. Gorkhover, I. Andersson, H. Hirsemann, G. Potdevin, H. Graafsma, B. Nilsson, J.C.H. Spence, Femtosecond X-ray protein nanocrystallography, Nature 470 (2011) 73–77.
[75] W. Liu, D. Wacker, C. Gati, G.W. Han, D. James, D. Wang, G. Nelson, U. Weierstall, V. Katritch, A. Barty, N.A. Zatsepin, D. Li, M. Messerschmidt, S. Boutet, G.J. Williams, J.E. Koglin, M.M. Seibert, C. Wang, S.T.A. Shah, S. Basu, R. Fromme, C. Kupitz, K.N. Rendek, I. Grotjohann, P. Fromme, R.A. Kirian, K.R. Beyerlein, T.A. White, H.N. Chapman, M. Caffrey, J.C.H. Spence, R.C. Stevens, V. Cherezov, Serial femtosecond crystallography of G protein-coupled receptors, Science 342 (2013) 1521–1524.
[76] R. Neutze, G. Brändén, G.F.X. Schertler, Membrane protein structural biology using X-ray free electron lasers, Curr. Opin. Struct. Biol. 33 (2015) 115–125.
[77] M.C. Wiener, Integral membrane proteins and free electron lasers – a compatible couple indeed, IUCrJ 2 (2015) 387–388.
[78] A.T. Tuukkanen, A. Spilotros, D.I. Svergun, Progress in small-angle scattering from biological solutions at high-brilliance synchrotrons, IUCrJ 4 (2017) 518–528.
[79] A. Berthaud, J. Manzi, J. Perez, S. Mangenot, Modeling detergent organization around aquaporin-0 using small-angle X-ray scattering, J. Am. Chem. Soc. 134 (2012) 10080–10088.
[80] O. Duss, E. Michel, M. Yulikov, M. Schubert, G. Jeschke, F.H.T. Allain, Structural basis of the non-coding RNA RsmZ acting as a protein sponge, Nature 509 (2014) 588–592.
[81] L.A. Earl, V. Falconieri, J.L.S. Milne, S. Subramaniam, Cryo-EM: beyond the microscope, Curr. Opin. Struct. Biol. 46 (2017) 71–78.
[82] K. Cosentino, S. Bleicken, A.J. García-Sáez, Analysis of Membrane-Protein Complexes by Single-Molecule Methods, Pumps, Channels, and Transporters, John Wiley & Sons, Inc., 2015, pp. 269–297.
[83] J. Ries, T. Weidemann, P. Schwille, Fluorescence correlation spectroscopy, in: E.H. Egelman (Ed.), Comprehensive Biophysics, Elsevier, 2012, pp. 210–245.
[84] H. Schneckenburger, Total internal reflection fluorescence microscopy: technical innovations and novel applications, Curr. Opin. Biotechnol. 16 (2005) 13–18.
[85] L.M.S. Loura, M. Prieto, FRET in membrane biophysics: an overview, Front. Physiol. 2 (2011) 82.
[86] D.W. Piston, G.-J. Kremers, Fluorescent protein FRET: the good, the bad and the ugly, Trends Biochem. Sci. 32 (2007) 407–414.
[87] E. Sisamakis, A. Valeri, S. Kalinin, P.J. Rothwell, C.A.M. Seidel, Chapter 18 - accurate single-molecule FRET studies using multiparameter fluorescence detection, Methods Enzymol. 475 (2010) 455–514.
[88] C.M. Grytz, S. Kazemi, A. Marko, P. Cekan, P. Guntert, S.T. Sigurdsson, T.F. Prisner, Determination of helix orientations in a flexible DNA by multi-frequency EPR spectroscopy, Phys. Chem. Chem. Phys. 19 (2017) 29801–29811.
[89] P.E. Czabotar, G. Lessene, A. Strasser, J.M. Adams, Control of apoptosis by the BCL-2 protein family: implications for physiology and therapy, Nat. Rev. Mol. Cell Biol. 15 (2014) 49–63.
[90] B. Favaloro, N. Allocati, V. Graziano, C. Di Ilio, V. De Laurenzi, Role of apoptosis in disease, Aging 4 (2012) 330–349.
[91] S. Bleicken, A.J. Garcia-Saez, E. Conte, E. Bordignon, Dynamic interaction of cBid with detergents, liposomes and mitochondria, PLoS One 7 (2012) e35910.
[92] F. Edlich, S. Banerjee, M. Suzuki, M.M. Cleland, D. Arnoult, C.X. Wang, A. Neutzner, N. Tjandra, R.J. Youle, Bcl-x(L) retrotranslocates Bax from the mitochondria into the cytosol, Cell 145 (2011) 104–116.
[93] B. Schellenberg, P. Wang, James A. Keeble, R. Rodriguez-Enriquez, S. Walker, T.W. Owens, F. Foster, J. Tanianis-Hughes, K. Brennan, Charles H. Streuli, Andrew P. Gilmore, Bax exists in a dynamic equilibrium between the cytosol and mitochondria to control apoptotic priming, Mol. Cell 49 (2013) 959–971.
[94] M. Suzuki, R.J. Youle, N. Tjandra, Structure of Bax: coregulation of dimer formation and intracellular localization, Cell 103 (2000) 645–654.
[95] S.W. Muchmore, M. Sattler, H. Liang, R.P. Meadows, J.E. Harlan, H.S. Yoon, D. Nettesheim, B.S. Chang, C.B. Thompson, S.L. Wong, S.L. Ng, S.W. Fesik, X-ray and NMR structure of human Bcl-xL, an inhibitor of programmed cell death, Nature 381 (1996) 335–341.
[96] J.J. Chou, H. Li, G.S. Salvesen, J. Yuan, G. Wagner, Solution structure of BID, an intracellular amplifier of apoptotic signaling, Cell 96 (1999) 615–624.
[97] S. Aluvila, T. Mandal, E. Hustedt, P. Fajer, J.Y. Choe, K.J. Oh, Organization of the mitochondrial apoptotic BAK pore: oligomerization of the BAK homodimers, J. Biol. Chem. 289 (2013) 2537–2551.
[98] T. Mandal, S. Shin, S. Aluvila, H.C. Chen, C. Grieve, J.Y. Choe, E.H. Cheng, E.J. Hustedt, K.J. Oh, Assembly of Bak homodimers into higher order homo-oligomers in the mitochondrial apoptotic pore, Sci. Rep. 6 (2016) 30763.
[99] S. Bleicken, M. Classen, P.V. Padmavathi, T. Ishikawa, K. Zeth, H.J. Steinhoff, E. Bordignon, Molecular details of Bax activation, oligomerization, and membrane insertion, J. Biol. Chem. 285 (2010) 6636–6647.
[100] T. Moldoveanu, Q. Liu, A. Tocilj, M. Watson, G. Shore, K. Gehring, The X-ray structure of a BAK homodimer reveals an inhibitory zinc binding site, Mol. Cell 24 (2006) 677–688.
[101] H. Li, H. Zhu, C.J. Xu, J. Yuan, Cleavage of BID by caspase 8 mediates the mitochondrial damage in the Fas pathway of apoptosis, Cell 94 (1998) 491–501.
[102] S. Desagher, A. Osen-Sand, A. Nichols, R. Eskes, S. Montessuit, S. Lauper, K. Maundrell, B. Antonsson, J.C. Martinou, Bid-induced conformational change of Bax is responsible for mitochondrial cytochrome c release during apoptosis, J. Cell Biol. 144 (1999) 891–901.
[103] S.J. Korsmeyer, M.C. Wei, M. Saito, S. Weiler, K.J. Oh, P.H. Schlesinger, Pro-apoptotic cascade activates BID, which oligomerizes BAK or BAX into pores that result in the release of cytochrome c, Cell Death Differ. 7 (2000) 1166–1173.
[104] T. Kuwana, L. Bouchier-Hayes, J.E. Chipuk, C. Bonzon, B.A. Sullivan, D.R. Green, D.D. Newmeyer, BH3 domains of BH3-only proteins differentially regulate Bax-mediated mitochondrial membrane permeabilization both directly and indirectly, Mol. Cell 17 (2005) 525–535.
[105] Peter E. Czabotar, D. Westphal, G. Dewson, S. Ma, C. Hockings, W.D. Fairlie, Erinna F. Lee, S. Yao, Adeline Y. Robin, Brian J. Smith, David C.S. Huang, Ruth M. Kluck, Jerry M. Adams, Peter M. Colman, Bax crystal structures reveal how BH3 domains activate Bax and nucleate its oligomerization to induce apoptosis, Cell 152 (2013) 519–531.
[106] D. Westphal, G. Dewson, M. Menard, P. Frederick, S. Iyer, R. Bartolo, L. Gibson, P.E. Czabotar, B.J. Smith, J.M. Adams, R.M. Kluck, Apoptotic pore formation is associated with in-plane insertion of Bak or Bax central helices into the mitochondrial outer membrane, Proc. Natl. Acad. Sci. U. S. A. 111 (2014) E4076–4085.
[107] S. Bleicken, O. Landeta, A. Landajuela, G. Basanez, A.J. Garcia-Saez, Proapoptotic Bax and Bak form stable protein-permeable pores of tunable size, J. Biol. Chem. 288 (2013) 33241–33252.
[108] J.F. Lovell, L.P. Billen, S. Bindner, A. Shamas-Din, C. Fradin, B. Leber, D.W. Andrews, Membrane binding by tBid initiates an ordered series of events culminating in membrane permeabilization by Bax, Cell 135 (2008) 1074–1084.
[109] T. Kuwana, M.R. Mackey, G. Perkins, M.H. Ellisman, M. Latterich, R. Schneiter, D.R. Green, D.D. Newmeyer, Bid, Bax, and lipids cooperate to form supramolecular openings in the outer mitochondrial membrane, Cell 111 (2002) 331–342.
[110] S.W. Tait, D.R. Green, Mitochondria and cell death: outer membrane permeabilization and beyond, Nat. Rev. Mol. Cell Biol. 11 (2010) 621–632.
[111] G. Jeschke, Conformational dynamics and distribution of nitroxide spin labels, Prog. Nucl. Magn. Reson. Spectrosc. 72 (2013) 42–60.
[112] A.W. Fischer, E. Bordignon, S. Bleicken, A.J. Garcia-Saez, G. Jeschke, J. Meiler, Pushing the size limit of de novo structure ensemble prediction guided by sparse SDSL-EPR restraints to 200 residues: the monomeric and homodimeric forms of BAX, J. Struct. Biol. 195 (2016) 62–71.
[113] Y. Subburaj, K. Cosentino, M. Axmann, E. Pedrueza-Villalmanzo, E. Hermann, S. Bleicken, J. Spatz, A.J. Garcia-Saez, Bax monomers form dimer units in the membrane that further self-assemble into multiple oligomeric species, Nat. Commun. 6 (2015) 8042.
[114] S. Iyer, F. Bell, D. Westphal, K. Anwari, J. Gulbis, B.J. Smith, G. Dewson, R.M. Kluck, Bak apoptotic pores involve a flexible C-terminal region and juxtaposition of the C-terminal transmembrane domains, Cell Death Differ. 22 (2015) 1665–1675.
[115] R.T. Uren, M. O'Hely, S. Iyer, R. Bartolo, M.X. Shi, J.M. Brouwer, A.E. Alsop, G. Dewson, R.M. Kluck, Disordered clusters of Bak dimers rupture mitochondria during apoptosis, elife 6 (2017) e19944.
[116] Z. Zhang, S. Subramaniam, J. Kale, C. Liao, B. Huang, H. Brahmbhatt, S.G. Condon, S.M. Lapolla, F.A. Hays, J. Ding, F. He, X.C. Zhang, J. Li, A. Senes, D.W. Andrews, J. Lin, BH3-in-groove dimerization initiates and helix 9 dimerization expands Bax pore assembly in membranes, EMBO J. 35 (2016) 208–236.
[117] S. Böhm, A. Licht, S. Wuttge, E. Schneider, E. Bordignon, Conformational plasticity of the type I maltose ABC importer, Proc. Natl. Acad. Sci. U. S. A. 110 (2013)

5492–5497.
[118] M. Majsnerowska, I. Hänelt, D. Wunnicke, Lars V. Schäfer, H.-J. Steinhoff, Dirk J. Slotboom, Substrate-induced conformational changes in the S-component ThiT from an energy coupling factor transporter, Structure 21 (2013) 861–867.
[119] P. Zou, H.S. McHaourab, Alternating access of the putative substrate-binding chamber in the ABC transporter MsbA, J. Mol. Biol. 393 (2009) 574–585.
[120] Smriti, P. Zou, H.S. McHaourab, Mapping daunorubicin-binding sites in the ATP-binding cassette transporter MsbA using site-specific quenching by spin labels, J. Biol. Chem. 284 (2009) 13904–13913.
[121] P.P. Borbat, K. Surendhran, M. Bortolus, P. Zou, J.H. Freed, H.S. McHaourab, Conformational motion of the ABC transporter MsbA induced by ATP hydrolysis, PLoS Biol. 5 (2007) e271.
[122] J. Dong, G. Yang, H.S. McHaourab, Structural basis of energy transduction in the transport cycle of MsbA, Science 308 (2005) 1023–1028.
[123] A. Mittal, S. Bohm, M.G. Grutter, E. Bordignon, M.A. Seeger, Asymmetry in the homodimeric ABC transporter MsbA recognized by a DARPin, J. Biol. Chem. 287 (2012) 20395–20406.
[124] T. Wiegand, D. Lacabanne, K. Keller, R. Cadalbert, L. Lecoq, M. Yulikov, L. Terradot, G. Jeschke, B.H. Meier, A. Böckmann, Solid-state NMR and EPR spectroscopy of Mn2 + -substituted ATP-fueled protein engines, Angew. Chem. Int. Ed. 56 (2017) 3369–3373.
[125] A. Collauto, S. Mishra, A. Litvinov, H.S. McHaourab, D. Goldfarb, Direct spectroscopic detection of ATP turnover reveals mechanistic divergence of ABC exporters, Structure 25 (2017) (1264-1274.e1263).
[126] A. Nöll, C. Thomas, V. Herbring, T. Zollmann, K. Barth, A.R. Mehdipour, T.M. Tomasiak, S. Brüchert, B. Joseph, R. Abele, V. Oliéric, M. Wang, K. Diederichs, G. Hummer, R.M. Stroud, K.M. Pos, R. Tampé, Crystal structure and mechanistic basis of a functional homolog of the antigen transporter TAP, Proc. Natl. Acad. Sci. U. S. A. 114 (2017) E438–E447.